Corrosion Inhibition and Acceleration by Rare Earth Ions in Galvanic Couples

M. Oliveira,[1] A. C. Bastos,[1,*,z] S. Kallip,[1,2] T. Hack,[3] M. L. Zheludkevich,[4] and M. G. S. Ferreira[1,]**

[1] *CICECO, Aveiro Institute of Materials and DEMaC, Department of Materials and Ceramic Engineering, University of Aveiro, 3810-193 Aveiro, Portugal*
[2] *Institute of Chemistry, University of Tartu, 50411, Tartu, Estonia*
[3] *AIRBUS, Central Research & Technology, 81663 Munich, Germany*
[4] *Institute of Materials Research, Helmholtz-Zentrum Geesthacht, Geesthacht 21502, Germany*

Rare earth ions are amongst the most promising new generation corrosion inhibitors. This communication describes conditions where, instead of inhibition, acceleration of corrosion occurs after rare earth salts are added to solution. The work was carried out mainly with the Fe-Zn galvanic couple and different rare earth salts, using electrochemical techniques such as galvanic current measurements, scanning vibrating electrode technique and linear sweep voltammetry (polarization curves). The increased activity in the couple is associated to an unexpected cathodic reaction that is observed after adding the salts to solution. The new reaction signifies supplementary oxidant species being reduced at the iron electrode (cathode), accelerating the oxidation of zinc (anode). The nature of this cathodic process is discussed.
 [DOI: 10.1149/2.0761916jes]

Manuscript submitted October 10, 2019; revised manuscript received December 3, 2019. Published December 19, 2019.

Since the first description of the reduced corrosion rate of AA7075 in solutions containing small concentrations of $CeCl_3$,[1,2] significant progress has been achieved in identifying new rare earth (RE) compounds with inhibiting properties, different forms of application, and other metals and alloys for which RE ions can efficiently reduce corrosion. In the following years various salts (chloride, nitrate, perchlorate, acetate, sulfate) of Ce, La, Y, Pr, Nd were investigated,[3–7] and complex compounds were synthesized, including dibutyl and diphenyl phosphates,[8] and rare earth carboxylate complexes (salicylate, anthranilate, glycolate and cinnamate).[9] From the initial additions to solution in low concentration,[1–5] RE compounds were soon tested in conversion coatings,[10–30] as sealants in anodizing,[31,32] inhibitive pigments for organic coatings[8,9,33] and, more recently, inside nano/micro-reservoirs for incorporation in paint formulations.[34–39] RE compounds were found to inhibit corrosion in aluminum alloys,[1,2,4,8,10,11,15,18–20,25,28,31–33,35–39] zinc and galvanized steel,[3,16,22,24,26,29,34,40] magnesium alloys,[13,21,23,27,30] mild and stainless steels.[9,12,14,17] The inhibition mechanism has been attributed to the reaction of RE ions with the OH^- ions generated at the cathodic sites, which produces a precipitated oxide/hydroxide layer, covering the cathodic area and blocking its activity.[1,41–44] A comprehensive account of the progress on the use of RE compounds for corrosion protection can be found in the book edited by Forsyth and Hinton.[45]

In the course of the investigation with RE ions, the present authors found many cases of successful corrosion inhibition using RE ions,[35,46–48] but also cases where corrosion was accelerated when RE ions were added to solution.[49] This communication analyzes and discusses the conditions for this acceleration. Following Hayes et al.,[50] in this work the term RE(III) refers to the oxidation state of RE in hydrolyzed or oxide form whereas RE^{3+} refers to species that are, at most, only weakly complexed with water.

Experimental

All solutions were prepared with distilled water and *pro analysis* grade reagents. Electrodes were made with pure metals (99.9+%, Goodfellow, UK) and carbon fiber reinforced plastic – (CFRP) – (65% Tenax HT 24 K carbon fiber in an epoxy vinyl matrix). The metal rods had diameters of 9.5 mm (Fe, Cu, Al) or 10 mm (Zn), and the CFRP rod had a diameter of 8 mm. Wires of 1 mm diameter (also from Goodfellow, UK) were used for the SVET measurements. The materials were cast in epoxy resin and the mount surfaces were abraded down to SiC P1200 grit paper, and finally rinsed with distilled water and ethanol.

Galvanic currents were measured with a zero-resistance ammeter (ZRA) using a Gamry Interface1000E + Gamry Framework software and are presented normalized by the cathode area. Polarization curves (linear sweep voltammograms) were obtained with a PGStat 302N Autolab potentiostat, at a scan rate of 1 mV s^{-1}, in a 3-electrode configuration, with pure iron or a 3 mm diameter platinum disk as working electrode, a platinum wire as counter electrode and a saturated calomel electrode (SCE) as reference. Some experiments were performed with a rotating ring disk electrode (RRDE.PTPT, both platinum) from Methrohm Autolab.

SVET measurements were performed with Applicable Electronics Inc.[51] equipment and controlled with the ASET software.[52] The SVET probe had a platinum black spherical tip of 10 μm in diameter, and vibrated with 5 μm amplitude and 89 Hz frequency in the direction normal to the surface. Maps with 50 × 50 points were acquired, 100 μm above the surface.

Local pH was measured with a potentiometric microelectrode comprising a borosilicate glass micropipette (6 cm long and 1.5 mm diameter) with one end thinned to ~ 2 μm diameter tip, filled with 0.1 M KCl + KH_2PO_4 0.01 M (internal solution), a silver|silver chloride wire as internal reference electrode and a ~ 25 μm column of pH selective gel (hydrogen I cocktail B ionophore, Fluka, Ref. 95293) at the tip. A homemade silver|silver chloride|0.05 M NaCl electrode served as external reference electrode. The pH microelectrode and the external reference electrode were connected to a pre-amplifier head (input resistance $>10^{15}$ Ω) mounted in the 3D positioning system used for SVET and connected to an IPA2 amplifier (input resistance > 10^{12} Ω) from Applicable Electronics. The microelectrode was calibrated before and after the measurements with commercial pH buffers, and presented a linear response in the 5 − 13 pH range with a slope of 54 mV per pH unit.

H_2 oxidation was measured with a Pt microelectrode using the IPA2 amplifier in the amperometric mode and a pre-amplifier for current detection produced by Applicable Electronics. The measurement was performed with two electrodes, a 10 μm diameter platinum microdisc in glass sheath (CH Instruments, USA, Ref. CHI100) as working electrode and a homemade Ag|AgCl|0.05 M NaCl electrode as counter/reference electrode, with the microdisk potential set to 0 V vs Ag|AgCl. More details about the localized techniques can be found in a previous work.[53]

*Electrochemical Society Member.
**Electrochemical Society Fellow.
[z]E-mail: acbastos@ua.pt

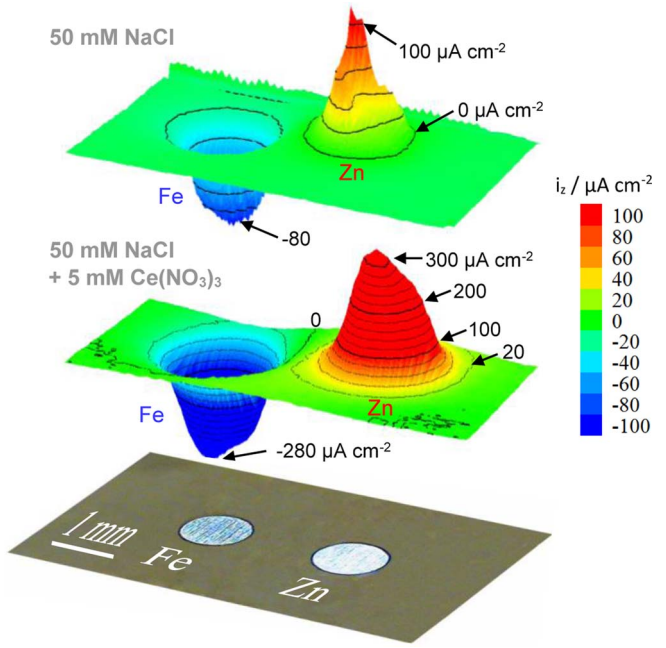

Figure 1. SVET maps with the current density (z component) measured 100 µm above a Fe-Zn galvanic couple in the first minutes of immersion in 50 mM NaCl without and with addition of $Ce(NO_3)_3$.

The measurements using microelectrodes were made above (5 µm for pH and 100 µm for H_2 oxidation) the center of a 1 mm diameter Pt disk electrode connected to an Ivium CompactStat potentiostat (SCE as reference and Pt wire as counter-electrode), which was powered by the laptop and disconnected from the mains power to avoid ground loops with the Applicable Electronics measuring station.

All measurements were performed at room temperature (23±1°C) inside a Faraday cage in quiescent and aerated conditions. In a few measurements, low oxygen conditions were achieved by purging the solution with argon for 30 minutes before the measurements.

Results and Discussion

Effect of cerium nitrate on the corrosion of the Fe-Zn galvanic couple.—In a previous work[49] performed by our group, Zn and Fe electrodes showed very low corrosion activity when immersed in 50 mM NaCl + 5 mM $Ce(NO_3)_3$ aqueous solution, but once they were electrically connected (externally) the galvanic current passing between the two was several times higher compared to the reference 50 mM NaCl solution. The experiments carried out with SVET were repeated in this work. A Fe-Zn galvanic couple was immersed in 50 mM NaCl, without and with cerium nitrate (corrosion inhibitor) at a concentration of 5 mM and SVET measured the *z* component of the current density flowing in solution, 100 µm above the couple. Figure 1 shows maps acquired during the first minutes of immersion. Anodic activity was observed on Zn and cathodic activity on Fe, as expected.[49,54–56] The currents were far much higher in the solution containing cerium nitrate which was in line with the previous observations,[49] but still not quite expected. These results denote an increase in corrosion rate where a decrease was expected due to the presence of inhibitor. The galvanic current flowing in the Fe-Zn couple during the first 12 hours of immersion is presented in Figure 2. The values measured after 30 minutes of immersion (around the time of the SVET measurements) were 43 µA cm^{-2} in NaCl and 251 µA cm^{-2} in the Ce(III) containing solution. After 12 hours the values decreased and were, respectively, 27 µA cm^{-2} and 184 µA cm^{-2}.

Effect of other rare earth salts.—Figure 2 also shows the galvanic currents of the Fe-Zn couple in solutions containing $CeCl_3$ and other

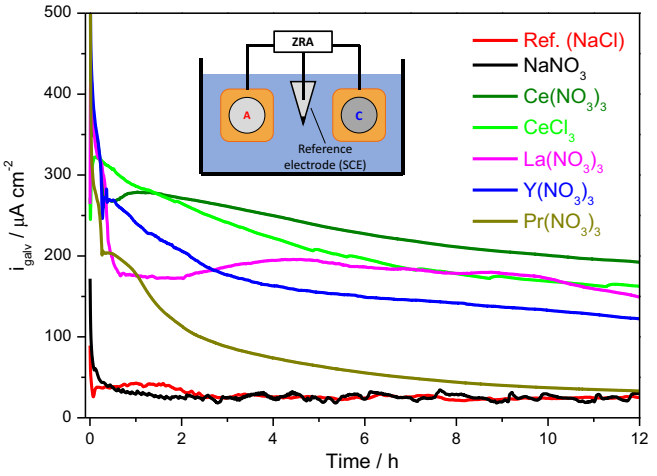

Figure 2. Galvanic currents flowing in the Fe-Zn couple during the first 12 hours of immersion in 50 mM NaCl + 5 mM RE(III) salts (15 mM $NaNO_3$).

RE salts, $La(NO_3)_3$, $Y(NO_3)_3$ and $Pr(NO_3)_3$. In all cases the galvanic currents were higher than in the reference NaCl solution (50 mM NaCl). $NaNO_3$ was also tested to exclude the possibility of the increased current coming from the presence of NO_3^-. The currents were measured at least in triplicate (see Figure S1 in Supplemental Material). Figure 3 presents the mean galvanic current after 30 minutes and 12 hours of immersion, the total charge passed during the 12 hours period and the corrosion potential of the couple after 12 hours of immersion. The increased current in $NaNO_3$ containing solution can be explained by the increase in its conductivity. With RE salts the currents were noticeably higher, being around 7 times greater in the case of Ce(III), compared to the reference solution. The corrosion potential of the couples was close to -1 V_{SCE} for NaCl and $CeCl_3$, and around -0.8 V_{SCE} for the systems with NO_3^-.

Linear sweep voltammetry.—To understand the galvanic currents obtained with the Fe-Zn couple, the response of the electrolyte solution was studied by linear sweep voltammetry with a platinum electrode (a comparison of curves obtained with iron and platinum electrodes are presented in Figure S2).

The first experiment was the cathodic sweep in the blank solution (0.05 M NaCl). The result is the red curve in Figure 4a, which is characterized by the reduction of dissolved oxygen dominating the plot until -0.9 V_{SCE} and then, at more negative potentials, the reduction of water with hydrogen evolution. The addition of cerium nitrate introduced a new wave, starting at around -0.7 V_{SCE}, with a limiting plateau. This wave was unexpected. This extra cathodic current can explain the higher galvanic currents observed in Figures 1 and 2. However, its origin is unknown. Some hypotheses are: i) reduction of nitrate, ii) reduction of RE(IV) after prior oxidation of RE(III), iii) reduction of RE(III), and iv) reduction of H^+ chemically generated by the hydrolysis of RE(III).

Hypothesis i) can be discarded because the wave does not appear when $NaNO_3$ is added to the NaCl solution, and is observed with cerium chloride, sulfate and acetate. The wave is also observed with La(III), Pr(III) and Y(III) – Figure 4b). Also important is the increase of the limiting current in an almost linear relationship with the concentration of RE(III), as shown in Figure 4c) for the case of Ce(III).

Hypothesis ii) can be refuted because there is not sufficient oxygen in solution to oxidize RE(III) to RE(IV), either directly or via H_2O_2, in order to sustain the extra reduction current. The concentration of dissolved O_2 in aqueous solution is around 0.25 mM.[57,58] The wave remains the same after decreasing the O_2 content in solution – Figure 4d. Moreover, this hypothesis cannot be applied to La or Y because La(IV) and Y(IV) have never been reported. Finally, the reduction of Ce(IV) to Ce(III) occurs at more positive potentials

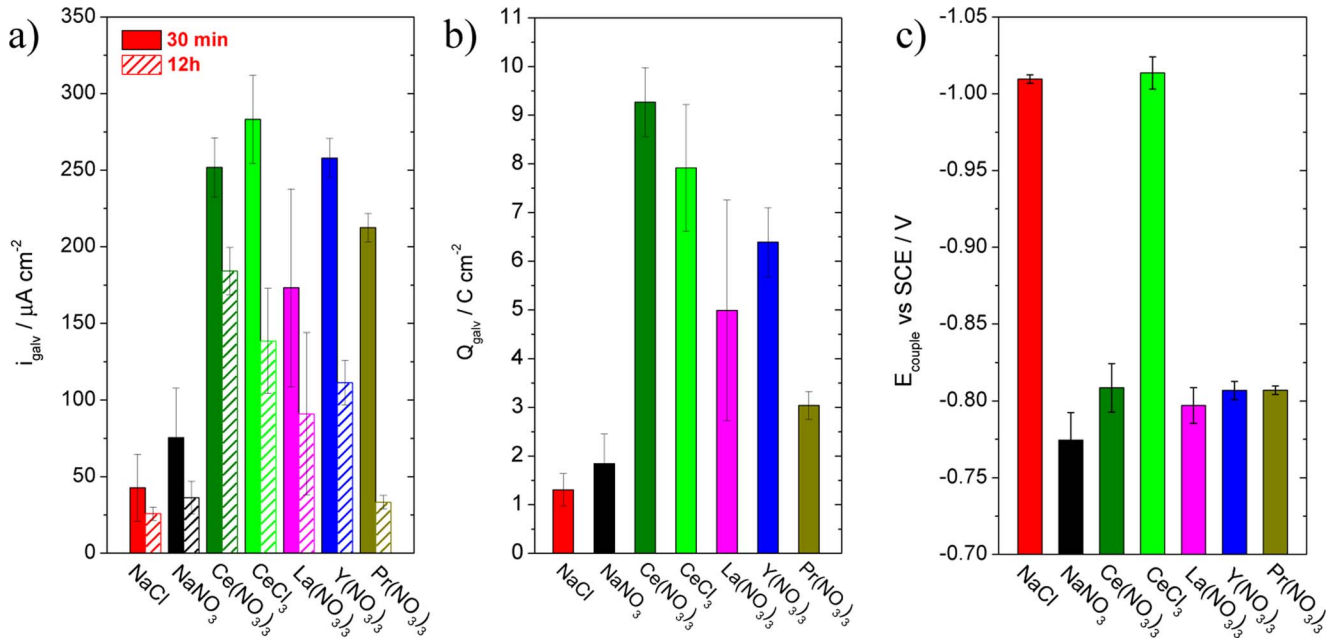

Figure 3. a) values of the galvanic current measured after 30 minutes and 12 hours of immersion; b) total charge passed in the 12 hours; c) corrosion potential measured after 12 hours of immersion. All values are mean values of at least 3 measurements (original curves in Supplemental Material).

(the standard potential is +1.74 V_{NHE} and the formal potential in 1 M H_2SO_4 is +1.44 V_{NHE}).[59,60] A few experiments were conducted with $Ce(SO_4)_2$ in solution – (Fig. 4e). The reagent was dissolved in 1 M H_2SO_4 to prevent the precipitation of Ce(IV) basic salts.[60] In such conditions, the voltammogram of 10 mM Ce(IV) solution showed the wave due to the reduction of Ce(IV) to Ce(III) starting close to +1 V_{SCE} and having a limiting current value of 1.3×10^{-4} A cm^{-2}. For comparison, the plot for $Ce(NO_3)_3$ is also depicted in Fig. 4e).

Hypothesis iii), reduction of RE(III), is also unlikely because lower oxidation states are very rare or have never been reported and the reduction to RE^0 takes place at very negative potentials.[59]

The fourth hypothesis is the reduction of H^+(aq), formed by hydrolysis of RE^{3+},

$$RE^{3+} + nH_2O \rightleftarrows RE(OH)_n^{(3-n)+} + nH^+ \quad [1]$$

The reduction of this H^+(aq) would give origin to a wave of hydrogen evolution at lower overpotentials.[61,62] Experiments performed to validate this hypothesis have failed. A wave was indeed produced in acidic solutions (pH 2–3) but it started at potentials between −0.3 V_{SCE} and −0.4 V_{SCE}, far from −0.7 V_{SCE} (Figure S3). In addition, even a 0.2 M Ce(III) solution has a pH not lower than 4.3 (Figure S4). The pH close (5 µm) to the electrode surface was measured with a microelectrode during the cathodic sweep – Figure 4f). No acidification was detected. The local pH increased in 0.05 M NaCl during the oxygen reduction and more after hydrogen evolution (E <−0.95 V_{SCE}). With Ce(III), the pH in the potential range dominated by the oxygen reduction did not rise above 5.8 – the produced OH^- reacted rapidly with Ce(III) – and increased only after water reduction started.

The hypothesis of reduction of water molecules in the hydration sphere of the rare earth cations.—All hypotheses raised in the previous section were proved incorrect. A similar wave, at the same potential as in this work, has been found in the literature for cathodic reactions on steel in aqueous solutions containing Y(III).[63] This wave was explained by the reduction of water molecules bound to yttrium aqua-complexes. Tran et al.[63] assumed that the Y···OH_2 coordination bond led to the weakening of the YOH···H bond in the water ligands of the coordination shell. As a result, the overpotential necessary for the reduction of the water-ligand was lower than that for the solvent water molecules. The proposed overall reaction was:

$$Y(H_2O)_x^{3+} + ne^- \rightleftarrows Y(H_2O)_{x-n}^{3+} + \frac{n}{2}H_2 + nOH^- \quad [2]$$

The work was continued and led to a publication describing the activation of water reduction in the presence of rare earth metal salts in aqueous solution.[64] Later, Gustavsson et al. reported the in-situ activation of hydrogen evolution in near-neutral pH electrolytes by addition of multivalent cations.[65] A reaction similar to 2 is believed to occur in this study, being responsible for the voltammetric wave at −0.7 V_{SCE}. In fact, the following conclusions from Gustavsson et al.[65] seem to describe well the results of Figure 4a: "The hydrogen evolution reaction can be activated by the electrolyte addition of trivalent metal ions. When adding the metal ions the reactant for hydrogen evolution changes from free water to water molecules complex bound to the metal ions, $M(H_2O)_x^{3+}$. Mass transport limitations for the activated hydrogen evolution reaction can be observed, as the metal ions are present at a much lower concentration than that of free water (about 55 M)".[65]

Further experiments were performed in an attempt to detect the formation of H_2 in the potential window between −0.7 V_{SCE} and −0.9 V_{SCE}. Figure 5a presents the current measured on the ring of a RRDE kept at constant potential E_{ring} = −0.5 V_{SCE} while potentiodynamic cathodic sweeps were carried out on the disk electrode – Figure 5b. The negative current measured on the ring comes from the reduction of dissolved oxygen in solution. It is smaller in the presence of Ce(III) due to the partial electrode hindrance by the precipitation of cerium oxides/hydroxides. At more negative potentials, the current becomes positive and is ascribed to the oxidation of H_2 that comes from the water reduction at the disk. For the blank solution, the current becomes positive at E_{disk} = −0.96 V_{SCE}. When Ce(III) is in solution, the onset of positive current happens before, at E_{disk} = −0.7 V_{SCE}, in agreement with an earlier oxidation of H_2. This H_2 oxidation current almost attains a plateau. Then, it increases for E_{disk} < −1 V_{SCE}, when the solvent water reduction adds to the existing bound water reduction. In another experiment – Figure 6 – a Pt microelectrode (10 µm diameter disk) was polarized at 0 V vs Ag|AgCl|50 mM NaCl and placed 100 µm above a Pt electrode (1 mm diameter disk) whose potential was swept in the negative direction with a scan rate of 1 mV s^{-1}. A positive current was measured by the microelectrode, starting at

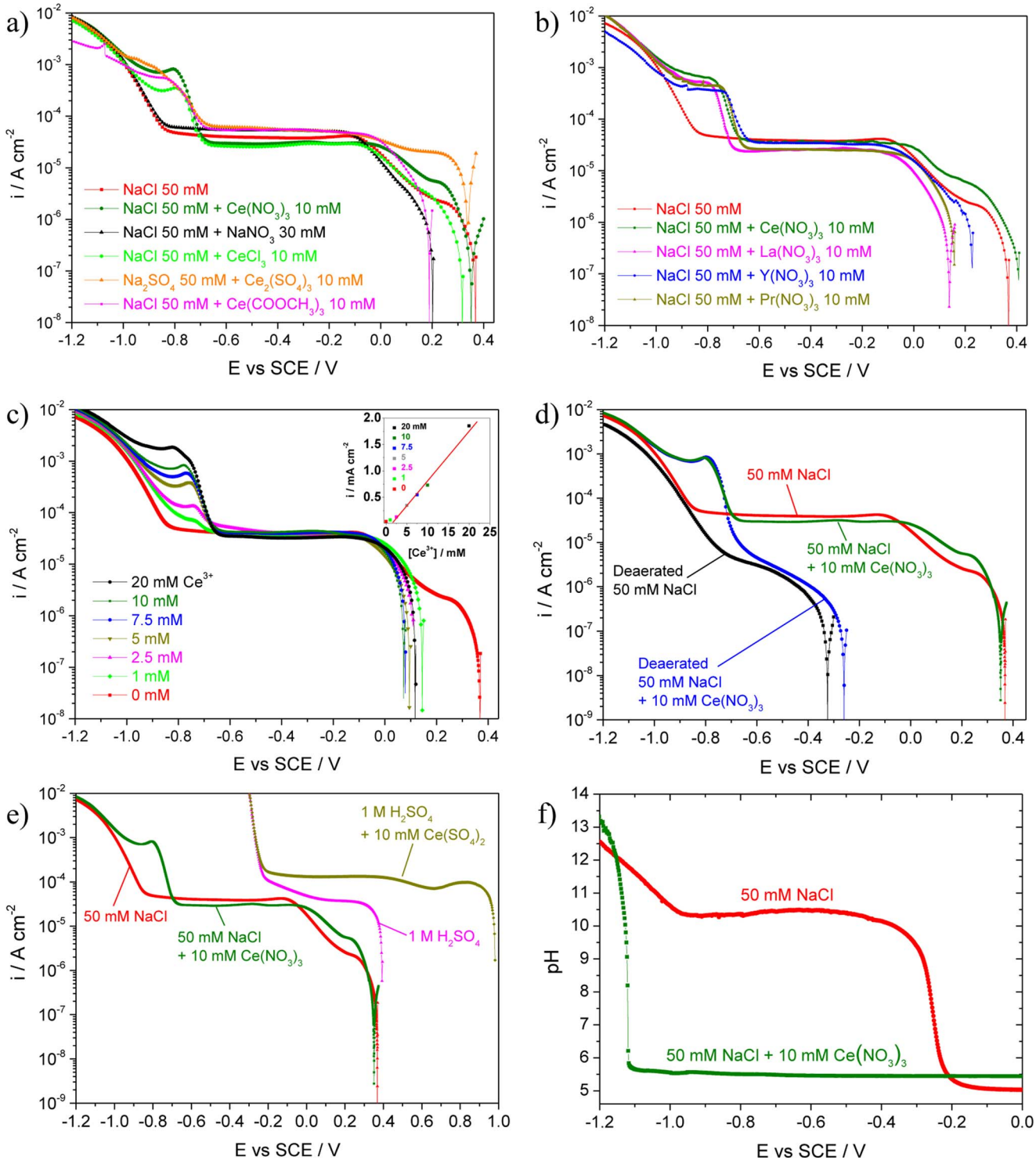

Figure 4. Cathodic voltammetric sweeps on platinum in 50 mM NaCl: a) with different Ce(III) salts, b) with other RE(III) ions, c) with varying concentration of $Ce(NO_3)_3$, d) in aerated and deaerated solution, e) with 10 mM Ce(IV) in 1 M H_2SO_4, f) pH measured 5 μm above the platinum surface during cathodic sweeps in 50 mM NaCl and 50 mM NaCl + 10 mM $Ce(NO_3)_3$.

substantially more positive potentials in the solution containing Ce(III), confirming the results of the previous experiment.

Both experiments show that the product of the reaction associated with the wave at −0.7 V_{SCE} diffuses away from the electrodes and is detected in the ring and in the microelectrode tip. The most likely candidate is H_2, as no Ce species in solution can be oxidized at this potential. For a direct verification of H_2 evolution, the potential of the 1 mm Pt disk was fixed at −0.8 V_{SCE} while the surface was monitored with a camera. A deposit was slowly formed at the surface – most likely Ce(III) oxides/hydroxides – and a small solution disturbance near the surface was detected in the video image, supposedly caused by gas evolution dispersed all over the surface, but without visualization of gas bubbles. After gently scratching the surface, gas bubbles immediately appeared – Figure 7. This is a direct identification of

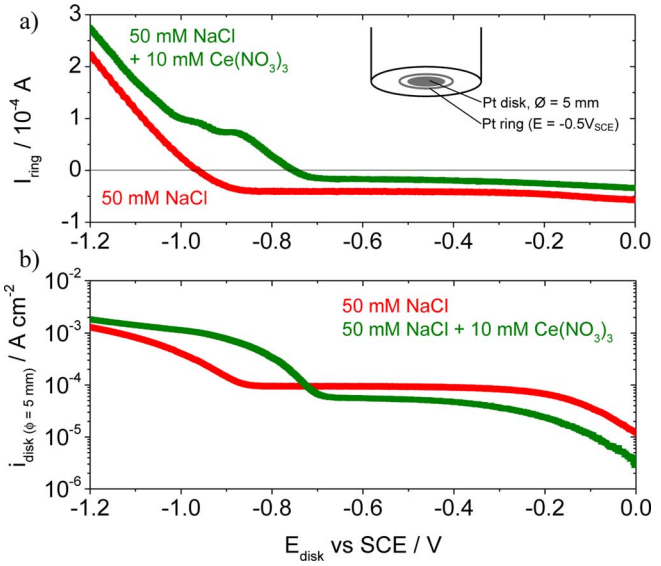

Figure 5. RRDE experiments in 50 mM NaCl and 50 mM NaCl + 10 mM $Ce(NO_3)_3$ (200 rpm). a) Current in the ring polarized at $E_{ring} = -0.5$ V_{SCE} while the disk is swept in the negative direction at a scan rate = 1 mVs^{-1}; b) current at the disk during the potentiodynamic sweeps.

hydrogen evolution at $-0.8V_{SCE}$ in a solution 50 mM NaCl + 10 mM $Ce(NO_3)_3$, confirming the hypothesis raised in this discussion. After a few seconds no further bubbles were formed. The scratched surface was slowly covered by a thin layer and the video image showed again small disturbance in solution above the electrode.

Inhibition vs acceleration.—This work showed an acceleration of the corrosion of the Fe-Zn couple in the presence of RE^{3+} ions. The acceleration comes from an extra cathodic process that appears when these ions are present in solution. A hypothesis about this reaction has been discussed above, but its exact identification is still yet to be confirmed.

It is clear that a galvanic potential of $E < -0.7$ V_{SCE} is a necessary condition for the acceleration. However, it is not sufficient. Zinc in

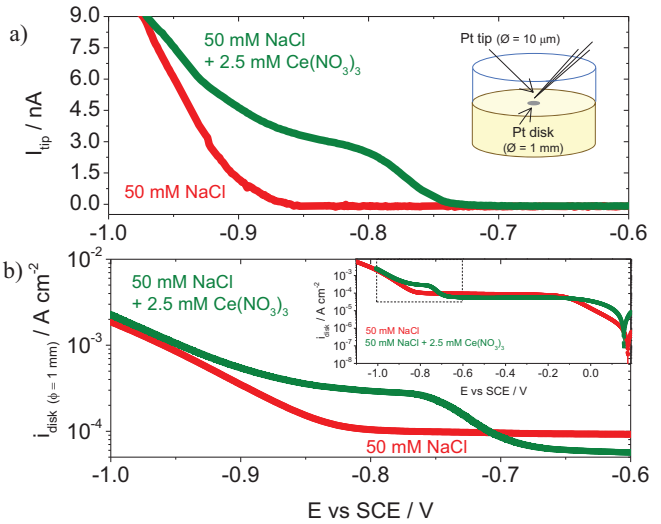

Figure 6. a) Current sensed by a 10 µm diameter Pt microelectrode polarized at 0 V vs Ag|AgCl|50 mM NaCl and placed 100 µm above the surface of a 1 mm Pt disk while it is swept in the negative direction at a scan rate = 1 mVs^{-1}, in 50 mM NaCl with and without 2.5 mM $Ce(NO_3)_3$; b) current at the disk during the potentiodynamic sweeps.

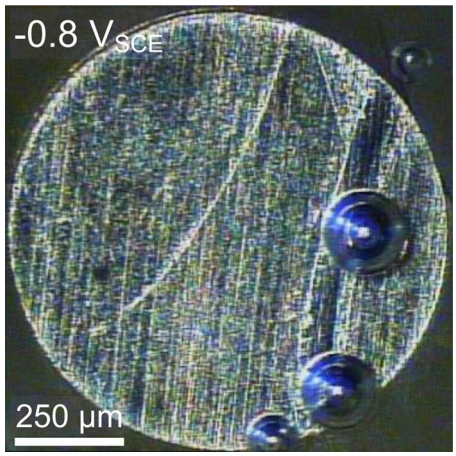

Figure 7. Pt disk immersed in 50 mM NaCl + 10 mM $Ce(NO_3)_3$, polarized at -0.8 V_{SCE} with formation of gas bubbles.

RE solutions lies within this potential range and has low corrosion rates.[3,16,22,24,26,29,34,40] The fact that inhibition ceases when coupled to iron suggests a competition between two processes involving RE^{3+} ions: one related to the precipitation of a RE oxide/hydroxide film that hinders the reacting surface, and another process that increases the cathodic current thus increasing the overall corrosion process. The actual conditions that favor one process or the other, and the consequent inhibition or acceleration of corrosion, remain undefined and are under investigation.

Other galvanic couples.—So far, this work has focused on the Zn-Fe galvanic couple. Other couples were tested to verify whether the observed effect also occurs with different galvanic combinations. Figure 8 shows the galvanic current, the charge passed in the cell, and the potential of the couple after 12 hours of immersion for the following galvanic couples: Zn-Fe (for comparison), Cu-Zn, CFRP-Zn, Fe-Al, CFRP-Al and Cu-Al. The presence of Ce(III) decreased the galvanic current in Fe-Al, CFRP-Al and Cu-Al. These couples showed corrosion potentials more positive than -0.7 V_{SCE}, therefore they do not satisfy the necessary condition for corrosion acceleration identified above. On the contrary, the couples with zinc meet that condition (the three have potentials more negative than -0.7 V_{SCE}). Corrosion is accelerated in Fe-Zn and Fe-Cu but not in CFRP-Zn. It seems that the extra reduction can proceed on copper, while it his hindered or is too slow on CFRP. This reveals another condition required for the acceleration. The kinetics of the cathodic reaction must be fast to have impact in the overall corrosion process. The kinetics depends on the catalytic properties of the cathode material for this reaction and also on the competition with the precipitation of RE oxides/hydroxides that might block the surface, hindering it for further reactions.

Final remarks.—The acceleration of galvanic corrosion by added chemical species expected to act as inhibitors has a tremendous practical impact. This is particularly important for galvanized steel, which is extensively used worldwide, and corresponds precisely to the galvanic couple studied in this work. The rare earth ions can initially reduce the degradation of the galvanized (Zn) layer, but once the steel base is exposed, the extra reduction reaction will increase the Zn consumption and significantly shorten the durability of the material.

Conclusions

RE^{3+} ions, commonly associated with cathodic inhibition, were observed to accelerate corrosion. The acceleration occurred in some galvanic couples with $E_{couple} < -0.7$ V_{SCE}. The rate increase is attributed to an additional reduction reaction that appears when RE^{3+} salts are added to solution. A hypothesis is raised that it corresponds

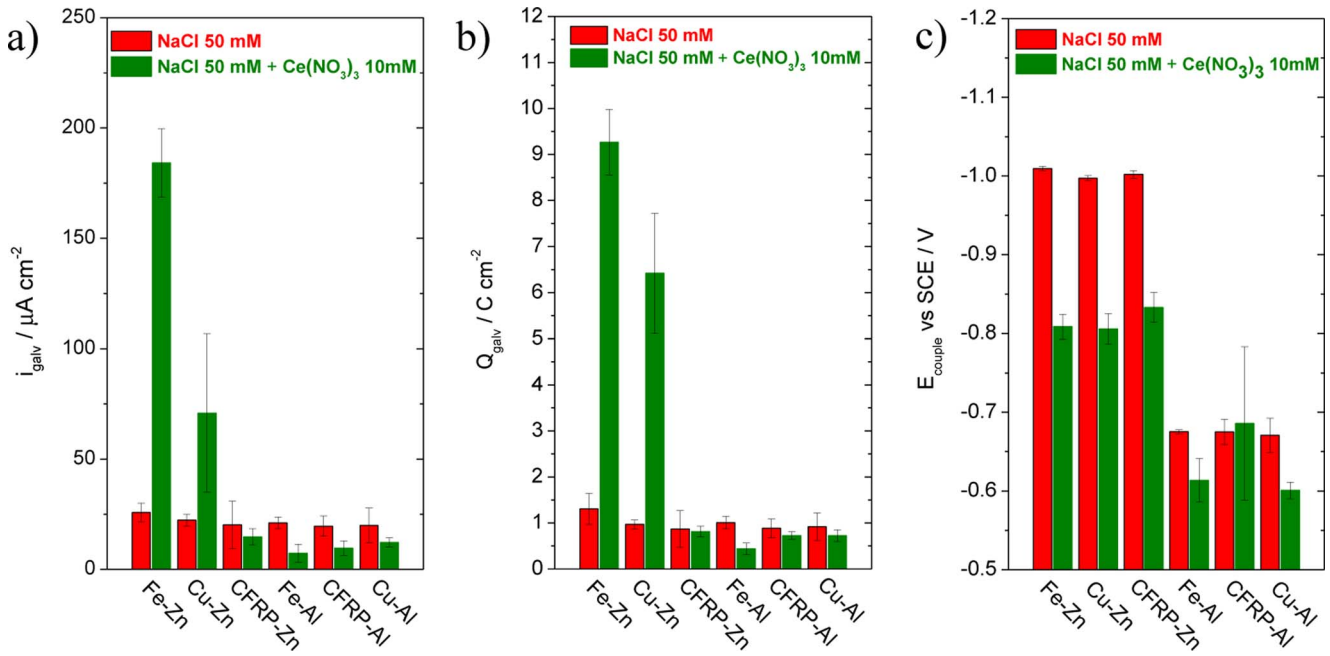

Figure 8. Results of various galvanic couples immersed in 50 mM NaCl and 50 mM NaCl + 10 mM $Ce(NO_3)_3$. a) Galvanic current measured after 12 hours of immersion; b) total charge passed in the 12 hours; c) corrosion potential measured after 12 hours of immersion. All values are mean values of at least 3 measurements.

to a pre-wave of hydrogen evolution due to the reduction of water molecules in the primary hydration sphere of RE^{3+} aqua-complexes. In spite of this extra reduction reaction, the corrosion acceleration is seldom detected and seems to occur under very specific circumstances that still need to be clarified.

Acknowledgments

This work was developed in the scope of the project CICECO – Aveiro Institute of Materials, POCI-01-0145-FEDER-007679 (Ref. FCT UID/CTM/50011/2013), financed by national funds through the FCT/MEC and when applicable co-financed by FEDER under the PT2020 Partnership Agreement. MO thanks FCT for the PhD grant SFRH/BD/117518/2016. ACB acknowledges FCT – Fundação para a Ciência e a Tecnologia, I.P., in the scope of the framework contract foreseen in the numbers 4, 5 and 6 of the article 23, of the Decree-Law 57/2016, of August 29, changed by Law 57/2017, of July 19. SK thanks FCT for grant (IF/00856/2013), ETAg for grant PUT1033 and ERA.NET for project RUS_ST2017-477 "ACTICOAT".

ORCID

M. Oliveira https://orcid.org/0000-0001-9264-6033
A. C. Bastos https://orcid.org/0000-0003-1847-2332
S. Kallip https://orcid.org/0000-0001-6093-3636
M. L. Zheludkevich https://orcid.org/0000-0002-9658-9619
M. G. S. Ferreira https://orcid.org/0000-0002-2071-9851

References

1. B. R. W. Hinton, D. R. Arnott, and N. E. Ryan, *Met. forum*, **7**, 211 (1984).
2. D. R. Arnott, N. E. Ryan, B. R. W. Hinton, B. A. Sexton, and A. E. Hughes, *Appl. Surf. Sci.*, **22–23**, 236 (1985).
3. B. R. W. Hinton and L. Wilson, *Corros. Sci.*, **29**, 967 (1989).
4. F. Mansfeld, S. Lin, S. Kim, and H. Shih, *J. Electrochem. Soc.*, **137**, 78 (1990).
5. B. R. W. Hinton, *J. Alloys Compd.*, **180**, 15 (1992).
6. B. R. W. Hinton, *Handbook on the Physics and Chemistry of Rare Earths,*, Chapter **140**, 1995, **21**, 29.
7. M. Bethencourt, F. J. Botana, J. J. Calvino, M. Marcos, and M. A. Rodríguez-Chacón, *Corros. Sci.*, **40**, 1803 (1998).
8. M. Forsyth, T. Markley, D. Ho, G. B. Deacon, P. Junk, B. Hinton, and A. Hughes, *Corrosion*, **64**, 191 (2008).
9. M. Forsyth, M. Seter, B. Hinton, G. Deacon, and P. Junk, *Austral. J. Chem.*, **64**, 812 (2011).
10. F. Mansfeld, S. Lin, S. Kim, and H. Shih, *Electrochim. Acta*, **34**, 1123 (1989).
11. F. Mansfeld, Y. Wang, and H. Shih, *Electrochim. Acta*, **37**, 2277 (1992).
12. F. Mansfeld, C. B. Breslin, A. Pardo, and F. J. Perez, *Surf. Coat. Tech.*, **90**, 224 (1997).
13. A. Rudd, C. B. Breslin, and F. Mansfeld, *Corr. Sci.*, **42**, 275 (2000).
14. M. Forsyth, K. Wilson, T. Behrsing, C. Forsyth, G. B. Deacon, and A. Phanasgoankar, *Corrosion*, **58**, 953 (2002).
15. P. Campestrini, H. Terryn, A. Hovestad, and J. H. W. de Wit, *Surf. Coat. Technol.*, **176**, 365 (2003).
16. M. A. Arenas and J. J. De Damborenea, *Electrochim. Acta*, **48**, 3693 (2003).
17. C. Wang, F. Jiang, and F. Wang, *Corros. Sci.*, **46**, 75 (2004).
18. C. Wang, F. Jiang, and F. Wang, *Corrosion*, **60**, 237 (2004).
19. A. Decroly and J.-P. Petitjean, *Surf. Coat. Technol.*, **194**, 1 (2005).
20. M. A. Conde, A. de Frutos, and J. de Damborenea, *Electrochim. Acta*, **53**, 7760 (2008).
21. K. Brunelli, M. Dabalà, I. Calliari, and M. Magrini, *Corros. Sci.*, **47**, 989 (2005).
22. M. Hosseini, H. Ashassi-Sorkhabi, and H. A. Y. Ghiasvand, *J. Rare Earths*, **25**, 537 (2007).
23. C. H. Liang and R. F. Zheng, *Mater. Corros.*, **58**, 193 (2007).
24. Y. Huang and F. Mansfeld, *Corrosion*, **65**, 507 (2009).
25. S. Kiyota, B. Valdez, M. Stoytcheva, R. Zlatev, and M. Scorr, *ECS Transactions*, **19**, 115 (2009).
26. T. Peng and R. Man, *J. Rare Earths*, **27**, 159 (2009).
27. X. Yang, G. Wang, G. Dong, F. Gong, and M. Zhang, *J. Alloys Compd.*, **487**, 64 (2009).
28. D. K. Heller, W. G. Fahrenholtz, and M. J. O'Keefe, *Corros. Sci.*, **52**, 360 (2010).
29. G. Kong, L. Liu, J. Lu, C. Che, and Z. Zhong, *J. Rare Earths*, **28**, 461 (2010).
30. S. Maddela, M. J. O'Keefe, Y.-M. Wang, and H.-H. Kuo, *Corrosion*, **66**, 115006 (2010).
31. F. Mansfeld, C. Chen, C. B. Breslin, and D. Dull, *J. Electrochem. Soc.*, **145**, 2792 (1998).
32. X. Yu, C. Yan, and C. Cao, *Mat. Chem. and Phys.*, **76**, 228 (2002).
33. K. R. Baldwin, M. C. Gibson, P. L. Lane, and C. J. E. Smith, The development of alternatives to chromate inhibitors for the protection of aerospace aluminum alloys, *7th European Symposium on Corrosion Inhibition*, University of Ferrara, pp. 771 (1990).
34. S. Bohm, H. N. McMurray, S. M. Powell, and D. A. Worsley, *Mater. Corros.*, **52**, 896 (2001).
35. M. L. Zheludkevich, R. Serra, M. F. Montemor, K. A.Yasakau, I. M. Miranda Salvado, and M. G. S. Ferreira, *Electrochim. Acta*, **51**, 208 (2005).

36. N. P. Tavandashti and S. Sanjabi, *Prog. Org. Coat.*, **69**, 384 (2010).
37. X. Jiang, Y.-B. Jiang, N. Liu, H. Xu, S. Rathod, P. Shah, and C. J. Brinker, *J. Nanomaterials*, Article ID 760237 (2011).
38. S. Kozhukharov, V. Kozhukharov, M. Wittmar, M. Schem, M. Aslan, H. Caparrotti, and M. Veith, *Prog. Org. Coat.*, **71**, 198 (2011).
39. S. A. S. Dias, S. V. Lamaka, C. A. Nogueira, T. C. Diamantino, and M. G. S. Ferreira, *Corros. Sci.*, **62**, 153 (2012).
40. K. Aramaki, *Corros. Sci.*, **43**, 2201 (2001).
41. A. J. Davenport, H. S. Isaacs, and M. W. Kendig, *Corros. Sci.*, **32**, 653 (1991).
42. A. J. Aldykewicz Jr, A. J. Davenport, and H. S. Isaacs, *J. Electrochem. Soc.*, **143**, 147 (1996).
43. F. Bin Li, R. C. Newman, and G. E. Thompson, *Electrochim. Acta*, **42**, 2455 (1997).
44. M. A. Arenas, M. Bethencourt, F. J. Botana, J. de Damborenea, and M. Marcos, *Corros. Sci.*, **43**, 157 (2001).
45. M. Forsyth and B. Hinton, Editors, *Rare Earth-Based Corrosion Inhibitors*, Woodhead Publishing (2014).
46. M. L. Zheludkevich, R. Serra, M. F. Montemor, and M. G. S. Ferreira, *Electrochem. Commun.*, **7**, 836 (2005).
47. A. C. Bastos, O. V. Karavai, M. L. Zheludkevich, K. A. Yasakau, and M. G. S. Ferreira, *Electroanalysis*, **22**, 2009 (2010).
48. K. A. Yasakau, J. Tedim, M. F. Montemor, A. N. Salak, M. L. Zheludkevich, and M. G. S. Ferreira, *J. Phys. Chem. C*, **117**, 5811 (2013).
49. S. Kallip, A. C. Bastos, K. A. Yasakau, M. L. Zheludkevich, and M. G. S. Ferreira, *Electrochem. Commun.*, **20**, 101 (2012).
50. S. A. Hayers, Y. Pu, T. J. O'Keefe, M. J. O'Keefe, and J. O. Stoffer, *J. Electrochem. Soc.*, **149**, C623 (2002).
51. www.applicableelectronics.com (accessed January **10**, 2019).
52. www.sciencewares.com (accessed January **10**, 2019).
53. A. C. Bastos, M. C. Quevedo, O. V. Karavai, and M. G. S. Ferreira, *J. Electrochem. Soc.*, **164**, C973 (2017).
54. Galvanic Corrosion and H. P. Hack, (Ed.), STP978, American Society for Testing and Materials, (1988).
55. K. Ogle, V. Baudu, L. Garrigues, and X. Philippe, *J. Electrochem. Soc.*, **147** 3654 (2000).
56. A. M. Simoes, A. C. Bastos, M. G. Ferreira, Y. Gonzalez-Garcia, S. Gonzalez, and R. M. Souto, *Corros. Sci.*, **49**, 726 (2007).
57. M. Hitchman, Measurements of Dissolved Oxygen, Vol. 49 of Chemical Analytical Chemistry and its Applications, John Wiley & Sons Inc., 1978.
58. O. Dolgikh, A. C. Bastos, A. Oliveira, C. Dan, and J. Deconinck, *Corros. Sci*, **102**, 338 (2016).
59. A. J. Bard, R. Parsons, and J. Jordan, Editors, *Standard Potentials in Aqueous Solution*, Marcel Dekker, New York (1985).
60. D. A. Skoog, D. M. West, and F. J. Holler, *Fundamentals of Analytical Chemistry*, 7th Ed, Saunders College Pub. (1996).
61. M. Stern, *J. Electrochem. Soc.*, **102**, 609 (1955).
62. G. K. H. Wiberg and M. Arenz, *Electrochim. Acta*, **158**, 13 (2015).
63. M. Tran, C. Fiaud, and E. M. M. Sutter, *J. Electrochem. Soc.*, **153**, B83 (2006).
64. M. Tran, P. Dubot, and E. M. M. Sutter, *Int. J. Hydrogen Energy*, **33**, 937 (2008).
65. J. Gustavsson, G. Lindbergh, and A. Cornell, *Int. J. Hydrogen Energy*, **37**, 9496 (2012).